

# Lipid Peroxidation Products Influence Calpain-1 Functionality In Vitro by Covalent Binding

Chaoyu Zhai, Steven M. Lonergan, Elisabeth J. Huff-Lonergan, Logan G. Johnson, Kitty Brown, Jessica E. Prenni, and Mahesh N Nair\*



Cite This: <https://doi.org/10.1021/acs.jafc.3c01225>



Read Online

ACCESS |

Metrics & More



Article Recommendations



Supporting Information

Downloaded via IOWA STATE UNIV on May 16, 2023 at 15:55:00 (UTC).  
See https://pubs.acs.org/sharingguidelines for options on how to legitimately share published articles.

**ABSTRACT:** The objective of the current study was to evaluate the effects of lipid peroxidation products, malondialdehyde (MDA), hexenal, and 4-hydroxynonenal (HNE), on calpain-1 function, and liquid chromatography and tandem mass spectrometry (LC-MS/MS) identification of adducts on calpain-1. Calpain-1 activity slightly increased after incubation with 100  $\mu\text{M}$  MDA but not with 500 and 1000  $\mu\text{M}$  MDA. However, calpain-1 activity was lowered by hexenal and HNE at 100, 500, and 1000  $\mu\text{M}$ . No difference in calpain-1 autolysis was observed between the control and 1000  $\mu\text{M}$  MDA. However, 1000  $\mu\text{M}$  hexenal and HNE treatments slowed the calpain-1 autolysis. Adducts of MDA were detected on glutamine, arginine, lysine, histidine, and asparagine residues via Schiff base formation, while HNE adducts were detected on histidine, lysine, glutamine, and asparagine residues via Michael addition. These results are the first to demonstrate that lipid peroxidation products can impact calpain-1 activity in a concentration-dependent manner and may impact the development of meat tenderness postmortem.

**KEYWORDS:** *calpain-1, lipid peroxidation products, post-translational modifications, proteolysis*

## INTRODUCTION

Calpains are a family of intracellular calcium-dependent cysteine proteases.<sup>1</sup> Calpain-1 and calpain-2 are heterodimers, which contain identical 28 kDa subunits and distinct 80 kDa subunits, and their activation requires the presence of both calcium and a reducing environment.<sup>1,2</sup> Both calpain-1 and calpain-2 activities significantly contribute to the proteolysis of cytoskeletal and myofibrillar proteins and the postmortem tenderization of meat.<sup>3–6</sup> Thus, these proteins play an important role in meat acceptability through tenderness development, a trait that significantly affects consumer satisfaction and, thus, the repeat of the purchase at the point of sale.<sup>7–9</sup>

Muscle tissue contains mono- and poly-unsaturated fatty acids, and oxidation of these during the postmortem period can lead to the formation of various aldehydes and ketones.<sup>10–12</sup> These lipid oxidation products are known to limit protein and enzyme functionality.<sup>13–15</sup> Some critical effects of these lipid oxidation products include impacts on meat color<sup>16</sup> and flavor.<sup>17</sup> Likewise, oxidative conditions generated by irradiation<sup>18</sup> and high-oxygen modified atmosphere packaging<sup>19</sup> (HiOx-MAP; 80% O<sub>2</sub>, 20% CO<sub>2</sub>) can also lower the proteolysis rate and tenderness in postmortem muscle during cold storage. These processes are often accompanied by increased lipid-derived aldehyde generation.<sup>19</sup> Calpain-1 activity and activation can be inhibited by reactive oxygen species, such as hydrogen peroxide<sup>2,20,21</sup> and nitric oxide.<sup>22</sup> However, the effect of covalent modification on calpain-1 functionality by lipid oxidation product adduction is not yet understood.

Protein lipoxidation refers to the post-translational modification of proteins by reactive or electrophilic lipid species.

Malondialdehyde (MDA; 3-carbon), hexenal (6-carbon), and 4-hydroxynonenal (HNE; 9-carbon) are lipid-oxidation-derived aldehydes that have been identified in fresh meat under aerobic packaging.<sup>11</sup> These aldehydes can cause protein lipoxidation by forming covalent bonds with proteins in meat,<sup>15,23,24</sup> and their reactivity varies with carbon number.<sup>13,14</sup> Therefore, the objective of the current study was to investigate the effect of lipid peroxidation products, MDA, hexenal, and HNE, on calpain-1 activity and autolysis in vitro coupled with liquid chromatography and tandem mass spectrometry (LC-MS/MS) identification of adducts on the protein. We hypothesized that calpain-1 activity would change after exposure to lipid peroxidation products, and these changes would be associated with the covalent binding of aldehydes on calpain-1.

## MATERIALS AND METHODS

**Purification of Calpain-1.** Calpain-1 was purified from porcine semimembranosus skeletal muscle using a method described by Thompson and Goll<sup>25</sup> with minor modifications detailed by Liu et al.<sup>26</sup> One unit of calpain-1 activity was defined as the amount necessary to generate an increase in absorbance of trichloroacetic acid-soluble peptides at 278 nm by one unit after 1 h of incubation with activity assay (40 mM Tris-HCl, 3.5 mg/mL casein, 5 mM

Received: February 26, 2023

Revised: April 21, 2023

Accepted: April 27, 2023

**Table 1.** Detected MDA Schiff Base Formation in Tryptic Peptides of Porcine Calpain-1 from both the Control Group and MDA Treatment (1000  $\mu$ M)

subunit and domain	MDA adduction site	peptide position and peptide sequence	projected protein residue accessibility	projected intramolecular noncovalent interaction on the side chain	substitution (MutPred2 score)
catalytic subunit, domain IIB	Lys(K)-229 <sup>a</sup>	229–240; KAPS <u>DLYSIILK</u>	accessible	hydrogen bond (Glu-226)	K229Y (0.714) K229F (0.722) K229W (0.693)
catalytic subunit, domain III	Asn(N)-367	365–376; NW <u>N</u> TTL <sup>Y</sup> EGTWR	accessible	hydrogen bond (Ser-515); hydrogen bond (Glu-516)	N367Y (0.451) N367F (0.386) N367W (0.438)
catalytic subunit, domain III	Arg(R)-473	472–481; ARSEQ <u>FINL</u> R	accessible	none	R473Y (0.615) R473F (0.561) R473W (0.504)
catalytic subunit, domain IV, EF-hand 1	Asn(N)-595	592–604; SMV <u>N</u> LMDRGNGK	accessible	none	N595Y (0.685) N595F (0.594) N595W (0.684)
regulatory subunit, domain VI, EF-hand 1 (helix)	Gln(Q)-105	101–124; RLFA <u>Q</u> LAGDDMEVSATELMNILNK	accessible	none	Q105Y (0.630) Q105F (0.678) Q105W (0.635)

<sup>a</sup>Adduction site showing deleterious effect (MutPred2 score  $\geq$  0.680) after substitutions with all three hydrophobic amino acids.

CaCl<sub>2</sub>, 0.1% MCE, pH 7.4 at 25 °C).<sup>27</sup> The purified calpain-1 used in the experiment had a specific activity of 60–70 units/mg protein.

**Influence of Lipid Oxidation Products on the Activity of Calpain-1.** The methodology described by Lametsch et al.<sup>21</sup> was utilized to determine the effects of MDA (Sigma-Aldrich), hexenal (trans-2-hexenal; TCI America), and HNE (Sigma-Aldrich) on calpain-1 activity. Pure calpain-1 (5  $\mu$ g) was dialyzed for 3 h against a TEM buffer (40 mM Tris-HCl pH 7.4, 1 mM ethylenediaminetetraacetic acid (EDTA), and 0.1%  $\beta$ -mercaptoethanol (MCE)) at 4 °C using Slide-A-Lyzer Mini dialysis units (molecular weight cutoff of 7000 Da; Pierce, Rockford, Illinois). Calpain-1 was then incubated with 100, 500, or 1000  $\mu$ M of MDA, hexenal, or HNE, or equal volumes of TEM (controls) buffer for 24 h at 4 °C. The MDA stock solution (10 mM) was prepared in ddH<sub>2</sub>O, while hexenal and HNE stock solutions (10 mM) were prepared in 100% ethanol. After incubation, the activity of calpain-1 was determined immediately in triplicate using the caseinolytic assay.<sup>27</sup> Each experiment was repeated six times ( $n = 6$ ). The activity of each oxidant treatment was expressed as a percentage of the activity of the control samples within each experiment. Twenty-four hours of incubation at 4 °C with less than 20% ethanol did not affect the calpain-1 activity in the current in vitro system.

**Influence of Lipid Oxidation Products on Autolysis of Calpain-1.** Pure calpain-1 (20  $\mu$ g) was dialyzed against TEM for 3 h at 4 °C. The dialyzed calpain was incubated with 1000  $\mu$ M treatments of MDA, hexenal, or HNE, or equal volumes of the solvent of oxidant stock solutions (controls) for 24 h at 4 °C. After incubation, 5  $\mu$ g of protein from each incubation was removed before adding CaCl<sub>2</sub>. Each preparation was then adjusted to 500  $\mu$ M CaCl<sub>2</sub> to initiate autolysis and incubated on ice for 15, 30, and 60 min. Autolysis was immediately arrested by adding a protein denaturing buffer containing 3% (wt/vol) sodium dodecyl sulfate (SDS), 30% (vol/vol) glycerol, 3 mM EDTA, 30 mM Tris-HCl, and 0.001% (wt/vol) pyronin Y, pH 8.0 and 0.1 volume of MCE.<sup>28</sup> Each sample was resolved on a 10% sodium dodecyl sulfate poly(acrylamide) gel electrophoresis (SDS-PAGE) gel in duplicate to evaluate the 80 kDa catalytic subunit autolysis. The control sample without CaCl<sub>2</sub> and the samples at 60 min autolysis from all treatments were resolved on a 15% SDS-PAGE gel in duplicate to evaluate 28 kDa regulatory subunit autolysis. Electrophoresis was run at a constant voltage of 90 V at 25 °C using Mini-PROTEAN systems (Bio-Rad). The gel running buffer

contained 25 mM Tris, 192 mM glycine, 2 mM EDTA, and 0.1% [w/v] SDS. All of the gels were visualized by silver staining following the manufacturer's instructions (FASTsilver Gel Staining Kit, Sigma-Aldrich) and imaged with an iBright CL750 imaging system (Invitrogen).

**LC-MS/MS Characterization of Oxidized Calpain-1.** Dialyzed calpain-1 (50  $\mu$ g) was incubated for 24 h at 4 °C with treatments of 1000  $\mu$ M of MDA, hexenal, or HNE, or equal volumes of the solvent of oxidant stock solutions (controls), followed by precipitation in methanol at –80 °C and centrifugation at 18,000g (4 °C) for 20 min. Samples were processed using the EasyPep Mini MS Sample Prep Kit (Thermo Fisher Scientific) following the manufacturer's instructions. Briefly, 50  $\mu$ g of precipitated protein was reconstituted in lysis buffer (100  $\mu$ L for each calpain sample). Reduction and alkylation solutions (EasyPep Mini MS Sample Prep Kit; Thermo Fisher Scientific) were sequentially added, followed by incubation at 95 °C for 10 min. After cooling to room temperature, 5  $\mu$ g of a Trypsin/Lys-C mixture was added, and samples were digested by shaking at 37 °C for 2.5 h. The enzymes were then deactivated with the Digestion Stop Solution, and contaminants were removed using mixed-mode peptide cleanup columns. The peptide eluate was dried in a vacuum evaporator and resuspended in 5% acetonitrile/0.1% formic acid. After solubilization, the absorbance at 205 nm was measured by a NanoDrop (Thermo Scientific). The total peptide concentration was subsequently calculated using an extinction coefficient of 31.<sup>29</sup>

Reverse-phase chromatography was performed by using water with 0.1% formic acid (A) and acetonitrile with 0.1% formic acid (B). An online enrichment column (Waters Symmetry Trap C18 100 Å, 5  $\mu$ m, 180  $\mu$ m ID  $\times$  20 mm) was used to purify and concentrate 0.75  $\mu$ g of peptides. A reverse-phase nanospray column (Waters, Peptide BEH C18; 1.7  $\mu$ m, 75  $\mu$ m ID  $\times$  150 mm, 45 °C) was used to perform subsequent chromatographic separation, using a 30 min gradient: 3–8% B over 3 min followed by 8–35% B over 27 min at a flow rate of 350 nL/min. Peptides were directly eluted into the mass spectrometer (Orbitrap Velos Pro, Thermo Scientific) equipped with a Nanospray Flex ion source (Thermo Scientific). Spectra were collected over a *m/z* range of 400–2000 under positive-mode ionization. Ions (+2 or +3) were accepted for MS/MS using a dynamic exclusion limit of 2 MS/MS spectra of a given *m/z* value for 30 s (exclusion duration of 90 s). The instrument was operated in the FT mode for MS detection with a resolution of 60,000 and in the ion trap mode for MS/MS detection

**Table 2.** Detected MDA Schiff Base Formation in Tryptic Peptides of Porcine Calpain-1 after MDA Treatment (1000  $\mu$ M)

subunit and domain	MDA adduction site	peptide position and peptide sequence	projected protein residue accessibility	projected intramolecular noncovalent interaction on the side chain	substitution (MutPred2 score)
catalytic subunit, domain I	Lys(K)-24	23–36; AKELGLGRHENA IK	accessible	hydrogen bond (Glu-372); ionic interaction (Glu-158)	K24Y (0.733) K24F (0.671) K24W (0.697)
catalytic subunit, domain I	Lys(K)-36 <sup>a</sup>	31–46; HENAI <u>K</u> YLGQDYEQLR	accessible	hydrogen bond (Asp-41)	K36Y (0.808) K36F (0.806) K36W (0.825)
catalytic subunit, domain IIB	Lys(K)-270 <sup>a</sup>	268–280; LV <u>K</u> GHAYSVTGAK	accessible	hydrophobic contact (Ile-254)	K270Y (0.812) K270F (0.784) K270W (0.804)
catalytic subunit, domain IIB, active site	His(H)-272 <sup>a</sup>	268–280; LV <u>K</u> G <u>H</u> AYSVTGAK	buried	weak hydrogen bond (Gln-109); hydrophobic contact (Val-269)	H272Y (0.897) H272F (0.898) H272W (0.931)
catalytic subunit, domain III	Lys(K)-398	386–400; NYPATFWVNPQ <u>F</u> KIR	buried	hydrogen bonds (Gln-456; Glu-493); hydrophobic contacts (Gln-522; Leu-524)	K398Y (0.551) K398F (0.591) K398W (0.577)
catalytic subunit, domain IV, EF-hand 2	Lys(K)-650	642–653; MAIESAG <u>F</u> KLNK	accessible	weak hydrogen bond (Gln-645)	K650Y (0.699) K650F (0.681) K650W (0.651)
regulatory subunit, domain VI, EF-hand 2 (helix)	Lys(K)-170	164–171; YLWNNN <u>I</u> KK	accessible	hydrogen bond (Asn-167)	K170Y (0.776) K170F (0.768) K170W (0.727)
regulatory subunit, domain VI, EF-hand 2 and 3 (helix)	Lys(K)-171 <sup>a</sup>	171–177; KW <u>Q</u> A <u>I</u> YK	accessible	hydrogen bond (Ala-199)	K171Y (0.764) K171F (0.815) K171W (0.803)
regulatory subunit, domain VI, EF-hand 3 (helix)	Lys(K)-177 <sup>a</sup>	172–183; W <u>Q</u> A <u>I</u> YK <u>Q</u> FDVDR	accessible	hydrogen bonds (Asp-131); hydrophobic contact (Leu-132)	K177Y (0.797) K177F (0.819) K177W (0.781)
regulatory subunit, domain VI, EF-hand 5 (helix)	Lys(K)-242 <sup>a</sup>	240–246; AF <u>K</u> SLDK	accessible	hydrogen bond (Tyr-74)	K242Y (0.822) K242F (0.831) K242W (0.815)

<sup>a</sup>Adduction sites showing deleterious effects (MutPred2 score  $\geq$  0.680) after substitutions with all three hydrophobic amino acids.

with the normalized collision energy set to 35%. Xcalibur 3.0 software (Thermo Scientific) was used to generate compound lists of the resulting spectra with an S/N threshold of 1.5 and 1 scan/group.

ProteoWizard MsConvert (version 3.0) was used to extract, deconvolute charge state, and deisotop tandem mass spectra. Mascot (Matrix Science, London, U.K.; version 2.6.0) was used to search for spectra from all samples against reverse concatenated databases. Databases were the Uniprot reference proteome for *Sus scrofa* (UP000008227 downloaded Jan 24, 2022) and cRAP (common contaminants downloaded on Oct 5, 2018). Mascot searched with a fragment ion mass tolerance of 0.80 Da and a parent ion tolerance of 20 PPM, assuming the digestion enzyme trypsin. To reduce search space, adducts were queried in separate Mascot tasks. Each task involved oxidation of methionine, and the adducts of interest on cysteine (Cys), lysine (Lys), histidine (His), arginine (Arg), glutamine (Gln), and asparagine (Asn) were set as variable modifications.<sup>30–36</sup>

Samples' search results were imported and combined using the probabilistic protein identification algorithms<sup>37</sup> implemented in the Scaffold software (version Scaffold\_5.1.2, Proteome Software Inc., Portland, OR).<sup>38</sup> Peptide thresholds were set as 90% based on hits to the reverse database.<sup>39</sup> Protein identifications were established at greater than 99.0% probability and contained at least two identified

peptides. The Protein Prophet algorithm was used to assign protein probabilities.<sup>40</sup> Proteins with similar peptides but that could not be differentiated based on MS/MS analysis alone were grouped to satisfy the principles of parsimony. Specifically, mass additions of 54<sup>35</sup> and 134 Da<sup>33,41</sup> were searched to identify MDA Schiff base formation and fluorescent DHP–lysine adduct, respectively. The mass increments for hexenal Schiff base adducts were 80 Da in nonreduced adducts and 82 Da in reduced adducts.<sup>42</sup> For hexenal Michael adducts, the mass increments were 98 Da in nonreduced adducts and 100 Da for the reduced adducts.<sup>42</sup> Pyridinium-type adducts (mass additions of 158 and 160 Da) of hexenal were also searched.<sup>42</sup> HNE Schiff base formation was searched with mass additions of 138 and 140 Da in nonreduced and reduced adducts, respectively.<sup>36,43,44</sup> HNE Michael adduct formation was searched with mass additions of 156 Da in nonreduced adducts and 158 Da for the reduced adducts.<sup>45</sup> A reported stable pyrrole-type HNE–lysine adduct (mass addition of 120 Da) was also searched.<sup>46</sup> The representative spectrum of adducted peptides and their fragmentation tables are included in the Supporting Materials.

**Adduction Annotation and Protein Variation Effect Analysis.** Identified adduction sites were annotated according to the porcine calpain-1 structure projected by the AlphaFold database (AF-P35750-F1 and AF-P04574-F1)<sup>47,48</sup> and visualized on the hetero-

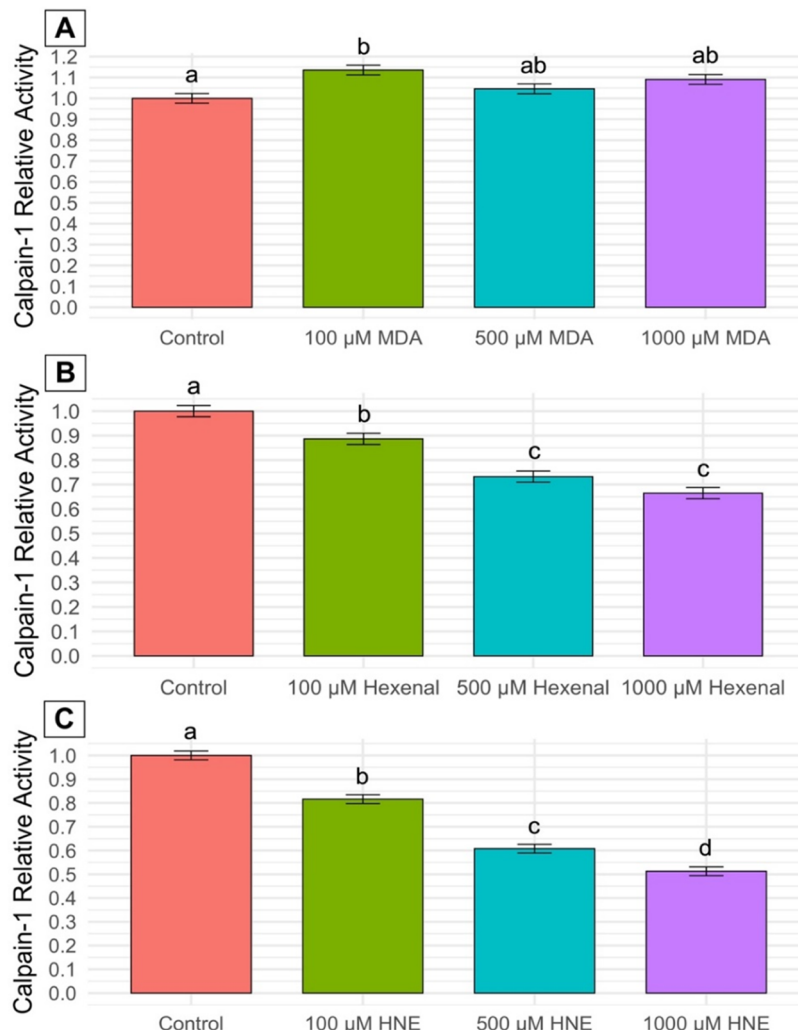


**Figure 1.** Effect of malondialdehyde (MDA; (A)), hexenal (B), and 4-hydroxynonenal (HNE; (C)) on purified porcine skeletal muscle calpain-1 activity ( $n = 6$ ) after 24 h incubation. The least-squares means for the enzyme activity of different treatments without a common letter (a–d) differ ( $P < 0.05$ ). Standard errors for the activity of calpain-1 after incubation with each lipid peroxidation product were: MDA = 0.0229, hexenal = 0.0186, HNE = 0.0234.

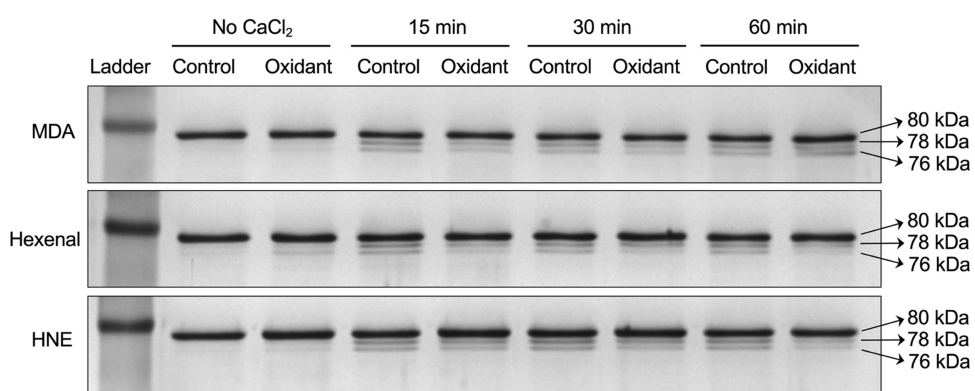


**Figure 2.** Progression of autolysis of the calpain-1 80 kDa catalytic subunit after exposure to various lipid oxidation products (malondialdehyde; MDA, hexenal, and 4-hydroxy-nonenal; HNE, 1000  $\mu$ M). The 80 kDa catalytic subunit undergoes autolysis from the N-terminus, resulting in the conversion of the 80 kDa subunit to a 76 kDa form through a 78 kDa intermediate.

meric complexes projected by ColabFold<sup>49</sup> (Figures 5 and 6). Detailed annotations of each adduction site, such as subunit, domain, amino acid, detected peptide position/peptide sequence, projected protein residue accessibility, and projected intramolecular non-covalent interaction of the side chain, are presented in Tables 1 and

2. MutPred2 was used to predict whether a side-chain adduction impacted the biological function<sup>50</sup> by substituting the adducted amino acid with three different hydrophobic amino acids (tyrosine, tryptophan, and phenylalanine). MutPred2 analysis filters side-chain variants to identify adduction sites predicted to be functionally

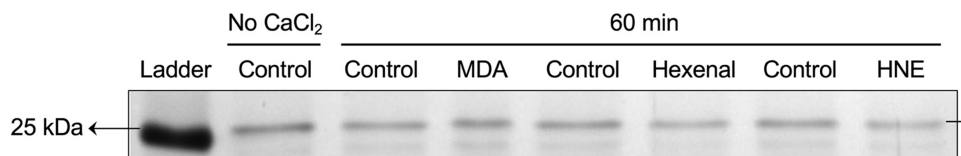


**Figure 3.** Sixty-minute autolysis of the calpain-1 28 kDa regulatory subunit after exposure to various lipid oxidation products (malondialdehyde; MDA, hexenal, and 4-hydroxy-nonenal; HNE, 1000  $\mu$ M).

important to calpain-1. The score threshold was set at 0.68 for binary classification (i.e., neutral: <0.680 vs deleterious:  $\geq$ 0.680) with a 10% false positive rate.<sup>50</sup> Adduction sites showing deleterious effects after substituting all three hydrophobic amino acids were identified.

**Statistical Analysis.** The effect of each lipid peroxidation product on calpain-1 relative activity was evaluated independently. A one-way analysis of variance (ANOVA) was conducted, followed by a least-square means test (em means function in R) to estimate the difference due to concentration ( $P < 0.05$ ).

## RESULTS AND DISCUSSION

**Effect of Each Lipid Peroxidation Product on Calpain-1 Activity and Autolysis.** The calpain-1 activity assay results after incubation with the lipid oxidation product under reducing conditions (0.1% MCE) are shown in Figure 1. Compared to the control, calpain-1 activity significantly increased after incubation with 100  $\mu$ M MDA ( $P < 0.05$ ; Figure 1A) but was not different after incubation with 500 and 1000  $\mu$ M MDA ( $P > 0.05$ ; Figure 1A). Incubations with hexenal (Figure 1B) and HNE (Figure 1C) significantly decreased calpain-1 activity at all three concentrations (100, 500, and 1000  $\mu$ M) compared to the control ( $P < 0.05$ ). Specifically, an inverse relationship was observed with a significant decrease in calpain-1 activity with increasing concentrations of hexenal (Figure 1B) and HNE (Figure 1C) from 100 to 1000  $\mu$ M ( $P < 0.05$ ).

There was no visible difference in the progression of the autolysis of the 80 kDa subunit of calpain-1 between control and MDA treatments; however, incubation with hexenal and HNE slowed down the autolysis of the 80 kDa subunit (Figure 2). In addition, no visible differences were observed in the autolysis of the 28 kDa subunit between the control and the lipid peroxidation product treatments (Figure 3).

Proteins are the principal molecular machines of the cell and derive their function from their amino acid sequence's unique three-dimensional folding structure.<sup>51</sup> The dominant contributors to protein folding include the hydrophobic effect, conventional hydrogen bonding, and Coulombic and van der Waals interactions.<sup>52</sup> However, additional contributors, such as strong interactions involving protein side chains, can also play an important role in protein folding.<sup>53</sup> Previous studies have demonstrated that MDA and HNE adducts on the side chain of an amino acid not only change the residue's chemical properties but also affect the interaction of this residue with the surrounding main chain, residues, and aqueous environment and, therefore, impacts protein functionality.<sup>54</sup>

The modification of proteins by electrophilic lipid peroxidation products occurs under basal conditions and increases in situations associated with oxidative stress.<sup>55,56</sup> In vitro MDA adducts have been identified in metabolic enzymes<sup>34</sup> and transport proteins.<sup>31</sup> Likewise, in vitro and in vivo HNE adducts have been identified in cytoskeletal proteins,<sup>57–59</sup> metabolic enzymes,<sup>60–62</sup> chaperones,<sup>63,64</sup> membrane receptors,<sup>65</sup> regulatory proteins,<sup>66,67</sup> signaling proteins,<sup>68–71</sup> and transport proteins.<sup>24,32,72</sup> The increased levels

of MDA and HNE adduction in proteins are also associated with acute and chronic diseases,<sup>55,73</sup> such as cardiovascular, Alzheimer's, Parkinson's, and liver diseases.

MDA is a standard compound used to evaluate lipid oxidation levels in meat using the thiobarbituric acid reactive substance method.<sup>74</sup> It is also well known that lipid oxidation products can compromise meat color stability<sup>13–15,23,75–77</sup> and flavor.<sup>17</sup> However, the effect of lipid peroxidation products on proteolytic enzymes is still an area with limited knowledge. Calpain-1 and 2 play a significant role in the postmortem proteolysis of cytoskeletal and myofibrillar proteins and in the postmortem tenderization of meat.<sup>3,5,6</sup> Calpain-1 is largely responsible for postmortem proteolysis during the early postmortem period.<sup>78</sup> During postmortem aging, calpain-1 can translocate from the sarcoplasm to myofibrils, and the myofibril-bound calpain-1 still has proteolytic activity.<sup>6</sup> Moreover, post-translational protein modification, such as *s*-nitrosylation<sup>79</sup> and oxidation,<sup>21,80</sup> has been demonstrated to impact calpain-1 activity.

The current study is the first to demonstrate that lipid peroxidation products (MDA, hexenal, and HNE) affect calpain-1 activity and autolysis *in vitro*. Specifically, HNE and hexenal decreased calpain-1 activity at all three concentrations compared to the control (100, 500, and 1000  $\mu$ M;  $P < 0.05$ ). Calpain-1 activity gradually decreased with the increase in the concentration of hexenal and HNE from 100 to 1000  $\mu$ M ( $P < 0.05$ ). However, calpain-1 still showed some proteolytic activity after incubation with 1000  $\mu$ M HNE or hexenal, which were approximately 51% and 66% of the control group activity, respectively. Interestingly, MDA did not decrease calpain-1 activity at any concentration. In fact, compared to the control, 100  $\mu$ M MDA slightly increased ( $P < 0.05$ ) calpain-1 activity (by about 13%). This increase became insignificant when the MDA concentration increased to 500 and 1000  $\mu$ M ( $P > 0.05$ ). Previous studies have shown that MDA adduction can inhibit the functionality of proteins, such as lactate dehydrogenase,<sup>13</sup> NADH-dependent metmyoglobin reductase,<sup>13</sup> and pyruvate kinase.<sup>34</sup> Although MDA further adducted on 11 different amino acid residues of calpain-1 after incubation with 1000  $\mu$ M MDA (Table 2), at this concentration, it did not decrease the calpain-1 activity *in vitro* compared to the control group. In contrast, in the current study, a significant decrease in calpain-1 activity was observed at all three concentrations (100, 500, and 1000  $\mu$ M) of HNE treatment. At 1000  $\mu$ M concentration, HNE further adducted on three amino acid residues in calpain-1 (Table 4), which was fewer than observed with MDA treatment. These results are consistent with previous studies<sup>13,34</sup> and indicated that HNE is more harmful to protein functionality than MDA at a similar concentration.

These observed activity changes were also reflected in the autolysis assay of calpain-1 after incubation with 1000  $\mu$ M MDA, hexenal, or HNE. In postmortem muscle, the presence of autolysis of calpain-1 is associated with the prior activity of

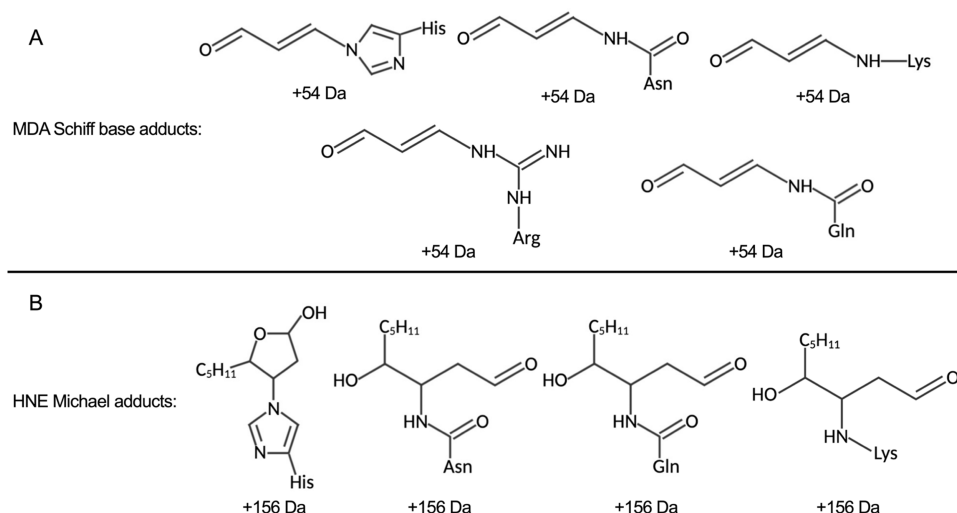
**Table 3.** Detected HNE Michael Addition in Tryptic Peptides of Porcine Calpain-1 from both the Control Group and HNE Treatment (1000  $\mu$ M)

subunit and domain	HNE adduction site	peptide position and peptide sequence	projected protein residue accessibility	projected intramolecular noncovalent interaction on the side chain	substitution (MutPred2 score)
regulatory subunit, domain VI, EF-hand 1 (helix)	Gln(Q)-105	102–124; LFA <u>QLAGDDMEVSATELMNILNK</u>	accessible	none	Q105Y (0.630) Q105F (0.678) Q105W (0.635)
regulatory subunit, domain VI, EF-hand 1 (helix)	Asn(N)-120	102–124; LFA <u>QLAGDDMEVSATELMN</u> ILNK	accessible	none	N120Y (0.593) N120F (0.579) N120W (0.648)
regulatory subunit, domain VI, EF-hand 1 (helix)	Lys(K)-124	102–124; LFA <u>QLAGDDMEVSATELMNILNK</u>	accessible	none	K124Y (0.602) K124F (0.653) K124W (0.593)

**Table 4.** Detected HNE Michael Addition in Tryptic Peptides of Porcine Calpain-1 after HNE Treatment (1000  $\mu$ M)

subunit and domain	HNE adduction site	peptide position and peptide sequence	projected protein residue accessibility	projected intramolecular noncovalent interaction on the side chain	substitution (MutPred2 score)
catalytic subunit, domain IIA	His(H)-179	175–193; LVFV <u>HSAQGNEFW</u> SALLEK	accessible	hydrophobic contact (Leu-175)	H179Y (0.527) H179F (0.623) H179W (0.681)
catalytic subunit, domain IIA	Gln(Q)-182	175–193; LVFV <u>HSAQGNEFW</u> SALLEK	accessible	none	Q182Y (0.440) Q182F (0.499) Q182W (0.396)
catalytic subunit, domain IIA	Asn(N)-184 <sup>a</sup>	175–193; LVFV <u>HSAQGNEFW</u> SALLEK	accessible	hydrogen bond (Asn-94)	N184Y (0.719) N184F (0.703) N184W (0.744)

<sup>a</sup>Adduction site showing deleterious effect (MutPred2 score  $\geq$  0.680) after substitutions with all three hydrophobic amino acids.

**Figure 4.** Predicted structures of identified MDA Schiff base formation (A) and HNE Michael addition (B) to amino acid residues in calpain-1 peptides.

calpain-1 and indicates that calpain has been active.<sup>81,82</sup> Calpain-1 autolysis is a calpain intermolecular event resulting in the cleavage of the 80 and 28 kDa subunits.<sup>83</sup> The 80 kDa catalytic subunit of calpain-1 undergoes autolysis from the N-terminus, resulting in its conversion to a 76 kDa form (through a 78 kDa intermediate) upon activation by  $\text{CaCl}_2$ .<sup>84,85</sup> There was no visible difference in 80 kDa subunit autolysis progression between the control and MDA treatment (Figure 2). Conversely, hexenal and HNE treatments appeared to slow down the autolysis of the 80 kDa subunit, especially in the 60

min samples (Figure 2). In general, both 78 and 76 kDa autolysis products were less visible in hexenal and HNE treatments as compared with the control treatment. The 78 and 76 kDa autolysis products were not different in the MDA treatment compared to the control (Figure 2). Importantly, calpain-1 showed autolysis regardless of oxidant treatment or concentration. This is consistent with the observation that while treatment with HNE and hexenal decreased calpain-1 activity, it did not inhibit calpain-1 activity. Autolysis of the calpain-1 28 kDa regulatory subunit was resolved on 15% SDS-

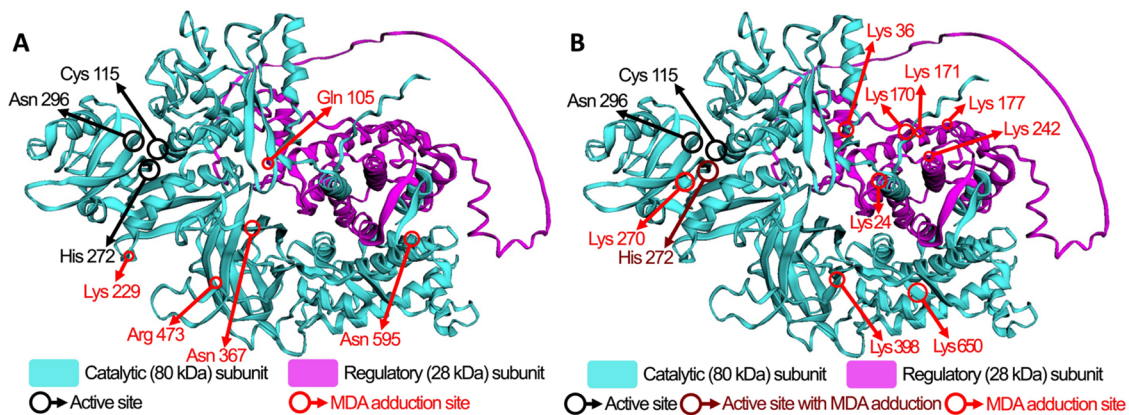


**Figure 5.** (A) Visualization of shared MDA adduction sites in the projected 3D structure of porcine calpain-1. (B) Visualization of additional adduction in the projected three-dimensional (3D) structure of porcine calpain-1 caused by 1000  $\mu\text{M}$  MDA incubation.

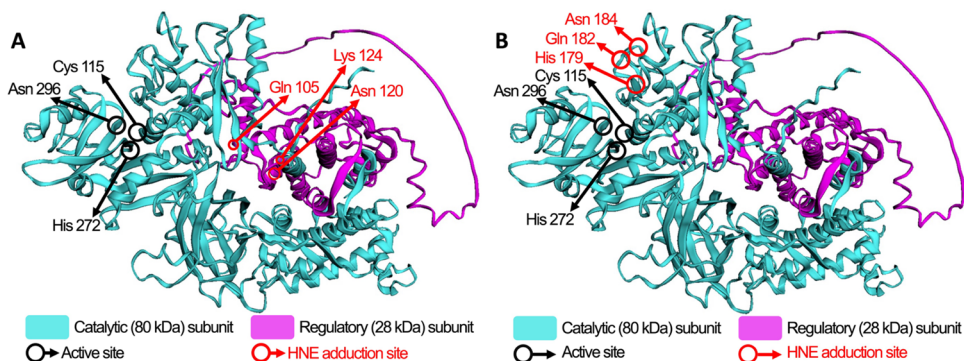


**Figure 6.** (A) Visualization of shared HNE adduction sites in the projected 3D structure of porcine calpain-1. (B) Visualization of additional adduction in the projected 3D structure of porcine calpain-1 caused by 1000  $\mu\text{M}$  HNE incubation.

poly(acrylamide) gel electrophoresis (SDS-PAGE) gels (Figure 3). It is known that autolysis of the 28 kDa regulatory subunit of calpain-1 to an 18 kDa product happens subsequent to autolysis of the 80 kDa subunit.<sup>84,85</sup> After 24 h incubation with 1000  $\mu\text{M}$  MDA, hexenal, and HNE and 60 min of autolysis after the addition of  $\text{CaCl}_2$ , there was no visible difference in the autolysis of the 28 kDa subunit between the control and any of the lipid peroxidation product treatments.

Previous studies have reported that calpain-1 activity and autolysis could be inhibited in postmortem muscle stored under an oxidizing environment,<sup>18,86,87</sup> a result that would account for the slower postmortem proteolysis and lower tenderness in meat under high-oxygen packaging than vacuum packaging.<sup>18,19,86,87</sup> However, it has also been demonstrated that the lipid-derived aldehyde formation is higher in high-oxygen packaging,<sup>19</sup> and the type of lipid peroxidation products formed during storage varies under different packaging systems.<sup>10,12,88</sup> Thus, based on the results of the current study, the reduced calpain-1 activity and tenderness in postmortem muscle under high-oxygen packaging compared to anaerobic packaging<sup>18,19,86,87</sup> could be partially attributed to the covalent reaction between lipid peroxidation products and calpain-1.

**Adducts of Lipid Peroxidation Products on Calpain-1.** The detailed annotations (subunit, domain, amino acid, detected peptide position/peptide sequence, projected protein residue accessibility, projected intramolecular noncovalent interaction of side chain, and MutPred2 score of each substitution) of detected MDA adduction sites are summarized

in Tables 1 and 2, and HNE adduction sites are summarized in Tables 3 and 4. MDA and HNE adduction sites are visualized in Figures 5 and 6, respectively.

Schiff base-type adducts of MDA were detected in calpain-1 from the control and treatment groups on the side-chain groups of Lys-229, Asn-367, Arg-473, and Asn-595 in the catalytic subunit as well as Gln-105 in the regulatory subunit (Figure 4A, Figure 5A, and Table 1). Incubation with 1000  $\mu\text{M}$  MDA further formed Schiff base-type adducts on the side-chain groups of Lys-24, Lys-36, Lys-270, His-272, Lys-398, and Lys-650 in the catalytic subunit as well as Lys-170, Lys-171, Lys-177, and Lys-242 in the regulatory subunit (Figure 4A, Figure 5B, and Table 2). Among these MDA adduction sites, His-272 and Lys-398 are the buried protein residues in the protein core, while the rest of the adduction sites are accessible amino acid residues on the protein surface. The MutPred2 score revealed that the adductions on Lys-36, Lys-229, Lys-270, and His-272 in the catalytic subunit and Lys-170, Lys-171, Lys-177, and Lys-242 in the regulatory subunit (Tables 1 and 2) have high confidence (score  $\geq 0.680$ ) and can impact calpain-1 functionality with substitution of all three amino acids.

Nonreduced Michael addition adducts of HNE were observed in calpain-1 from the control and treatment groups on the side chains of Gln-105, Asn-120, and Lys-124 in the regulatory subunit (Figure 4B, Figure 6A, and Table 3). Incubation with 1000  $\mu\text{M}$  HNE further formed adducts on His-179, Gln-182, and Asn-184 in the catalytic subunit via Michael addition (nonreduced; Figure 4B, Figure 6B, and

**Table 4**). All HNE adduction sites are accessible on the protein surface. The MutPred2 score revealed that the adductions on Asn-184 in the catalytic subunit have a high confidence (score  $\geq 0.680$ ) in affecting calpain-1 functionality. Hexenal-adducted peptides were not identified in the current study.

**Shared Adduction in Calpain-1 between Control and Treatment Samples.** Schiff base-type adducts of MDA were detected in calpain-1 from both control and MDA ( $1000 \mu\text{M}$ ) treatments on the side-chain groups of Lys-229, Asn-367, Arg-473, and Asn-595 in the catalytic subunit as well as Gln-105 in the regulatory subunit (Figure 4A, Figure 5A, and Table 1). Nonreduced Michael additions of HNE were detected in calpain-1 from both control and HNE ( $1000 \mu\text{M}$ ) treatments on the side-chain groups of Gln-105, Asn-120, and Lys-124 in the regulatory subunit (Figure 4B, Figure 6A, and Table 3). Hexenal-adducted peptides were not identified in the current study. This could be attributed to the neutral loss of adducts during collision-induced dissociation,<sup>64,89</sup> which inhibited the efficient fragmentation needed for peptide identification. Future studies using alternative fragmentation methods may enable the detection of intact adducts of hexenal on calpain-1 amino acid residues. To our knowledge, the current study is the first to report lipid peroxidation products' adduction sites to calpain-1. Notably, these adductions were shared between the control and MDA or HNE treatment. Further studies are necessary to characterize these adducts *in vivo* and understand their effect on calpain-1 functionality.

**Additional Adduction in Calpain-1 Caused by MDA and HNE Incubation.** After incubation with  $1000 \mu\text{M}$  MDA, six additional adduction sites of MDA were detected on the catalytic subunit (Lys-24, Lys-36, Lys-270, His-272, Lys-398, and Lys-650), and four were detected on the regulatory subunit (Lys-170, Lys-171, Lys-177, and Lys-242; Figure 5B, Table 2). Based on the MutPred2 score ( $\geq 0.680$ ), the adductions on Lys-36, Lys-270, and His-272 in the catalytic subunit (Table 2) and Lys-170, Lys-171, Lys-177, and Lys-242 in the regulatory subunit (Table 2) were projected to be the most significant for the changes in calpain-1 functionality. Lys-36 has an accessible side chain located in domain I of the catalytic subunit, which is projected to have a hydrogen bond with buried Asp-41. Lys-270 has an accessible side chain in domain IIB of the catalytic subunit, which is projected to have hydrophobic contact with accessible Ile-254. His-272 is one of the three amino acids (Cys-115, His-272, and Asn-296) composing the active site in porcine calpain-1 whose side chain is buried in domain IIB of the catalytic subunit. This His-272 side chain is projected to have a weak hydrogen bond with buried Gln-109 and a hydrophobic contact with buried Val-269. Lys-170, Lys-171, and Lys-177 have accessible side chains in domain VI of the regulatory subunit, the helix structure of EF-hand 3. Lys-170 and Lys-171 are projected to have hydrogen bonds with accessible Asn-167 and buried Ala-199, respectively. Also, Lys-177 is projected to have two hydrogen bonds with accessible Asp-131 and hydrophobic contact with buried Leu-132. Lys-242 has an accessible side chain located in domain VI of the regulatory subunit, the helix structure of EF-hand 5, which is projected to have a hydrogen bond with buried Tyr-74.

Interestingly, two of these amino acids (His-272 and Lys-398) are projected to be buried in the internal space of the calpain-1 molecular structure, which theoretically gives limited access to molecules, like MDA, for covalent binding. Therefore, these two adductions might be the result of

covalent binding occurring subsequent to MDA adductions on other accessible amino acid residues. The initial MDA adduct formation would alter the protein tertiary structure, making some buried residues, including His-272 and Lys-398, accessible to the potent electrophile in the surrounding environment. Cys-115 (the active site of calpain-1) is located in domain IIA, while the other two (His-272 and Asn-296) are in domain IIB. Upon calcium ions binding to protease core sites, salt bridges that maintain the "open configuration" will be disrupted, resulting in the active configuration of the active site; the three components of the active site will come together and result in proteolytic activity.<sup>90</sup> A previous study demonstrated that oxidation of the active site (Cys-115) leads to the reversible loss of calpain-1 activity.<sup>21</sup> Likewise, MDA adduct formation on the side chain of His-272 could make this residue hydrophobic and decrease the proteolytic activity. In our calpain-1 activity data (Figure 1), incubation with  $100 \mu\text{M}$  MDA increased calpain-1 activity *in vitro* by about 13%. However, higher concentration treatments of MDA ( $500$  and  $1000 \mu\text{M}$ ) did not result in a change of calpain-1 activity. This result suggests that there may be dynamic protein folding changes caused by the cumulative adduction of MDA to calpain-1 when the MDA concentration increases. According to the adduction annotation and protein variation effect analysis (i.e., neutral:  $< 0.680$  vs deleterious:  $\geq 0.680$ ; Table 2), Lys-36 and Lys-270 in the catalytic subunit as well as Lys-170, Lys-171, Lys-177, and Lys-242 in the regulatory subunit are the accessible amino acids projected to have the greatest impact on calpain-1 protein functionality. Notably, Lys-270 is spatially close to His-272 (Figure 5B). Adduct formation on the side chain of Lys-270 could affect the spatial proximity of Lys-270 to His-272, leading to changes in protein folding and protein functionality. Specifically, it is possible that adduction of MDA from a low-concentration treatment ( $100 \mu\text{M}$ ) changed the protein tertiary structure by altering the noncovalent interaction with near amino acid residues and the aqueous environment, resulting in an increased calpain-1 activity and exposure of the His-272 residue to the surrounding environment. When the MDA treatment concentration was increased to  $1000 \mu\text{M}$ , additional adduction of MDA on His-272 compromised the subtly increased activity and did not impact calpain-1 activity overall. Future studies are necessary to confirm this possibility.

After incubation with  $1000 \mu\text{M}$  HNE, three additional adduction sites were detected on the catalytic subunit (His-179, Gln-182, and Asn-184; Figure 6B and Table 2). All HNE-adducted amino acids in calpain-1 are accessible. Among these amino acids, the adduction on Asn-184 in the catalytic subunit was projected to be the most significant for the changes in calpain-1 functionality (Table 4). Asn-184 is an accessible amino acid located in domain IIA of the catalytic subunit and is projected to have a hydrogen bond with accessible Asn-94. Similar to what was observed with MDA adduction, HNE adduction to the Asn-184 side chain made this amino acid more hydrophobic. This could change the protein tertiary structure through the noncovalent interaction with nearby amino acids and the aqueous environment, explaining the observed decrease in calpain-1 activity. Again, additional studies are needed to confirm this possibility.

The current study is the first to demonstrate that lipid peroxidation products have differential impacts on calpain-1 activity in a concentration-dependent manner *in vitro*. Incubation with hexenal and HNE decreased the calpain-1

activity and the autolysis rate, whereas incubation with MDA slightly increased the calpain-1 activity. MDA adducts were detected on glutamine, arginine, lysine, histidine, and asparagine residues of calpain-1 via Schiff base formation, while HNE adducts were detected on lysine, histidine, glutamine, and asparagine residues via Michael addition. These results lay the groundwork for future investigations to understand the mechanistic basis of these differences, including their impacts on calpain activity in postmortem muscle and the development of meat tenderness.

## ■ ASSOCIATED CONTENT

### Data Availability Statement

Raw LC-MS/MS data have been deposited to the MassIVE database ([doi: 10.25345/C56M3380J](https://doi.org/10.25345/C56M3380J)) with the identifier MSV000090726.

### SI Supporting Information

The Supporting Information is available free of charge at <https://pubs.acs.org/doi/10.1021/acs.jafc.3c01225>.

Representative spectrum of adducted peptides and their fragmentation tables ([PDF](#))

## ■ AUTHOR INFORMATION

### Corresponding Author

Mahesh N Nair — Department of Animal Sciences, Colorado State University, Fort Collins, Colorado 80523, United States;  [orcid.org/0000-0002-2917-1028](https://orcid.org/0000-0002-2917-1028); Email: [mnaair@colostate.edu](mailto:mnaair@colostate.edu)

### Authors

Chaoyu Zhai — Department of Animal Science, University of Connecticut, Storrs, Connecticut 06269, United States; Department of Animal Sciences, Colorado State University, Fort Collins, Colorado 80523, United States

Steven M. Lonergan — Department of Animal Science, Iowa State University, Ames, Iowa 50011, United States

Elisabeth J. Huff-Lonergan — Department of Animal Science, Iowa State University, Ames, Iowa 50011, United States

Logan G. Johnson — Department of Animal Science, Iowa State University, Ames, Iowa 50011, United States;

 [orcid.org/0000-0001-9773-5027](https://orcid.org/0000-0001-9773-5027)

Kitty Brown — Analytical Resources Core-Bioanalysis & Omics, Colorado State University, Fort Collins, Colorado 80523, United States

Jessica E. Prenni — Department of Horticulture and Landscape Architecture, Colorado State University, Fort Collins, Colorado 80523, United States;  [orcid.org/0000-0002-0337-8450](https://orcid.org/0000-0002-0337-8450)

Complete contact information is available at:

<https://pubs.acs.org/doi/10.1021/acs.jafc.3c01225>

### Funding

This work was partially supported by the USDA National Institute of Food and Agriculture, Multi-State Hatch project COL00276B, accession number 7003980. This experiment was also partially supported by Iowa Agriculture and Home Economics Experiment Station (IAHEES) Project Proposal for Project No. IOW04121.

### Notes

The authors declare no competing financial interest.

## ■ ACKNOWLEDGMENTS

The authors acknowledge that Dr. Ed Steadham carried out all of the calpain purifications. The acquisition and analysis of mass spectrometry data utilized RRID SCR\_021758.

## ■ REFERENCES

- (1) Goll, D. E.; Thompson, V. F.; Li, H.; Wei, W.; Cong, J. The Calpain System. *Physiol. Rev.* **2003**, *83*, 731–801.
- (2) Guttmann, R. P.; Elce, J. S.; Bell, P. D.; Isbell, J. C.; Johnson, G. V. W. Oxidation Inhibits Substrate Proteolysis by Calpain I but Not Autolysis. *J. Biol. Chem.* **1997**, *272*, 2005–2012.
- (3) Koohmariae, M. Biochemical Factors Regulating the Toughening and Tenderization Processes of Meat. *Meat Sci.* **1996**, *43*, 193–201.
- (4) Koohmariae, M.; Geesink, G. H. Contribution of Postmortem Muscle Biochemistry to the Delivery of Consistent Meat Quality with Particular Focus on the Calpain System. *Meat Sci.* **2006**, *74*, 34–43.
- (5) Lyu, J.; Ertbjerg, P. Ca<sup>2+</sup>-Induced Binding of Calpain-2 to Myofibrils: Preliminary Results in Pork Longissimus Thoracis Muscle Supporting a Role on Myofibrillar Protein Degradation. *Meat Sci.* **2021**, *172*, No. 108364.
- (6) Lyu, J.; Ertbjerg, P. Sarcoplasmic and Myofibril-Bound Calpains during Storage of Pork Longissimus Muscle: New Insights on Protein Degradation. *Food Chem.* **2022**, *372*, No. 131347.
- (7) Grunert, K. G.; Bredahl, L.; Brunsø, K. Consumer Perception of Meat Quality and Implications for Product Development in the Meat Sector—a Review. *Meat Sci.* **2004**, *66*, 259–272.
- (8) Shackelford, S. D.; Wheeler, T. L.; Meade, M. K.; Reagan, J. O.; Byrnes, B. L.; Koohmariae, M. Consumer Impressions of Tender Select Beef. *J. Anim. Sci.* **2001**, *79*, 2605–2614.
- (9) Troy, D. J.; Kerry, J. P. Consumer Perception and the Role of Science in the Meat Industry. *Meat Sci.* **2010**, *86*, 214–226.
- (10) Jääskeläinen, E.; Hultman, J.; Parshtsev, J.; Riekkola, M.-L.; Björkroth, J. Development of Spoilage Bacterial Community and Volatile Compounds in Chilled Beef under Vacuum or High Oxygen Atmospheres. *Int. J. Food Microbiol.* **2016**, *223*, 25–32.
- (11) Lynch, M. P.; Faustman, C.; Silbart, L. K.; Rood, D.; Furr, H. C. Detection of Lipid-Derived Aldehydes and Aldehyde:Protein Adducts In Vitro and in Beef. *J. Food Sci.* **2008**, *66*, 1093–1099.
- (12) Lyte, J. M.; Legako, J. F.; Martin, J. N.; Thompson, L.; Surowiec, K.; Brooks, J. C. Volatile Compound Characterization of Modified Atmosphere Packaged Ground Beef Held under Temperature Abuse. *Food Control* **2016**, *59*, 1–6.
- (13) Zhai, C.; Peckham, K.; Belk, K. E.; Ramanathan, R.; Nair, M. N. Carbon Chain Length of Lipid Oxidation Products Influence Lactate Dehydrogenase and NADH-Dependent Metmyoglobin Reductase Activity. *J. Agric. Food Chem.* **2019**, *67*, 13327–13332.
- (14) Faustman, C.; Liebler, D. C.; McClure, T. D.; Sun, Q. α,β-Unsaturated Aldehydes Accelerate Oxymyoglobin Oxidation. *J. Agric. Food Chem.* **1999**, *47*, 3140–3144.
- (15) Ramanathan, R.; Mancini, R. A.; Suman, S. P.; Beach, C. M. Covalent Binding of 4-Hydroxy-2-Nonenal to Lactate Dehydrogenase Decreases NADH Formation and Metmyoglobin Reducing Activity. *J. Agric. Food Chem.* **2014**, *62*, 2112–2117.
- (16) Faustman, C.; Sun, Q.; Mancini, R.; Suman, S. P. Myoglobin and Lipid Oxidation Interactions: Mechanistic Bases and Control. *Meat Sci.* **2010**, *86*, 86–94.
- (17) Ponce, J.; Brooks, J. C.; Legako, J. F. Chemical Characterization and Sensory Relationships of Beef M. Longissimus Lumborum and M. Gluteus Medius Steaks After Retail Display in Various Packaging Environments. *Meat Muscle Biol.* **2020**, *4*, 1–17.
- (18) Rowe, L. J.; Maddock, K. R.; Lonergan, S. M.; Huff-Lonergan, E. Oxidative Environments Decrease Tenderization of Beef Steaks through Inactivation of μ-Calpain. *J. Anim. Sci.* **2004**, *82*, 3254–3266.
- (19) Vierck, K. R.; Legako, J. F.; Kim, J.; Johnson, B. J.; Brooks, J. C. Determination of Package and Muscle-Type Influence on Proteolysis, Beef-Flavor-Contributing Free Amino Acids, Final Beef Flavor, and Tenderness. *Meat Muscle Biol.* **2020**, *4*, 1–14.

- (20) Carlin, K. R. M.; Huff-Lonergan, E.; Rowe, L. J.; Lonergan, S. M. Effect of Oxidation, PH, and Ionic Strength on Calpastatin Inhibition of  $\mu$ - and m-Calpain. *J. Anim. Sci.* **2006**, *84*, 925–937.
- (21) Lametsch, R.; Lonergan, S.; Huff-Lonergan, E. Disulfide Bond within M-Calpain Active Site Inhibits Activity and Autolysis. *Biochim. Biophys. Acta, Proteins Proteomics* **2008**, *1784*, 1215–1221.
- (22) Li, Y.-p.; Liu, R.; Zhang, W.; Fu, Q.; Liu, N.; Zhou, G. Effect of Nitric Oxide on  $\mu$ -Calpain Activation, Protein Proteolysis, and Protein Oxidation of Pork during Post-Mortem Aging. *J. Agric. Food Chem.* **2014**, *62*, 5972–5977.
- (23) Suman, S. P.; Faustman, C.; Stamer, S. L.; Liebler, D. C. Proteomics of Lipid Oxidation-Induced Oxidation of Porcine and Bovine Oxymyoglobins. *Proteomics* **2007**, *7*, 628–640.
- (24) Wang, Y.; Li, S.; Rentfrow, G.; Chen, J.; Zhu, H.; Suman, S. P. Myoglobin Post-Translational Modifications Influence Color Stability of Beef Longissimus Lumborum. *Meat Muscle Biol.* **2021**, *5*, 1–21.
- (25) Thompson, V. F.; Goll, D. E. Purification of Mu-Calpain, m-Calpain, and Calpastatin from Animal Tissues. *Methods Mol. Biol.* **2000**, *144*, 3–16.
- (26) Liu, R.; Lonergan, S.; Steadham, E.; Zhou, G.; Zhang, W.; Huff-Lonergan, E. Effect of Nitric Oxide and Calpastatin on the Inhibition of M-Calpain Activity, Autolysis and Proteolysis of Myofibrillar Proteins. *Food Chem.* **2019**, *275*, 77–84.
- (27) Koohmaraie, M. Quantification of Ca<sup>2+</sup>-Dependent Protease Activities by Hydrophobic and Ion-Exchange Chromatography. *J. Anim. Sci.* **1990**, *68*, 659–665.
- (28) Huff-Lonergan, E.; Mitsuhashi, T.; Parrish, F. C., Jr; Robson, R. M. Sodium Dodecyl Sulfate-Polyacrylamide Gel Electrophoresis and Western Blotting Comparisons of Purified Myofibrils and Whole Muscle Preparations for Evaluating Titin and Nebulin in Postmortem Bovine Muscle. *J. Anim. Sci.* **1996**, *74*, 779–785.
- (29) Scopes, R. K. Measurement of Protein by Spectrophotometry at 205 Nm. *Anal. Biochem.* **1974**, *59*, 277–282.
- (30) Esterbauer, H. Cytotoxicity and Genotoxicity of Lipid-Oxidation Products. *Am. J. Clin. Nutr.* **1993**, *57*, 779S–786S.
- (31) Ishii, T.; Ito, S.; Kumazawa, S.; Sakurai, T.; Yamaguchi, S.; Mori, T.; Nakayama, T.; Uchida, K. Site-Specific Modification of Positively-Charged Surfaces on Human Serum Albumin by Malondialdehyde. *Biochem. Biophys. Res. Commun.* **2008**, *371*, 28–32.
- (32) Isom, A. L.; Barnes, S.; Wilson, L.; Kirk, M.; Coward, L.; Darley-Usmar, V. Modification of Cytochrome c by 4-Hydroxy-2-Nonenal: Evidence for Histidine, Lysine, and Arginine-Aldehyde Adducts. *J. Am. Soc. Mass Spectrom.* **2004**, *15*, 1136–1147.
- (33) Lamore, S. D.; Azimian, S.; Horn, D.; Anglin, B. L.; Uchida, K.; Cabello, C. M.; Wondrak, G. T. The Malondialdehyde-Derived Fluorophore DHP-Lysine Is a Potent Sensitizer of UVA-Induced Photooxidative Stress in Human Skin Cells. *J. Photochem. Photobiol. B* **2010**, *101*, 251–264.
- (34) Sousa, B. C.; Ahmed, T.; Dann, W. L.; Ashman, J.; Guy, A.; Durand, T.; Pitt, A. R.; Spickett, C. M. Short-Chain Lipid Peroxidation Products Form Covalent Adducts with Pyruvate Kinase and Inhibit Its Activity in Vitro and in Breast Cancer Cells. *Free Radicals Biol. Med.* **2019**, *144*, 223–233.
- (35) Uchida, K.; Sakai, K.; Itakura, K.; Osawa, T.; Toyokuni, S. Protein Modification by Lipid Peroxidation Products: Formation of Malondialdehyde-DerivedNe-(2-Propenal)Lysine in Proteins. *Arch. Biochem. Biophys.* **1997**, *346*, 45–52.
- (36) Zhao, J.; Chen, J.; Zhu, H.; Xiong, Y. L. Mass Spectrometric Evidence of Malonaldehyde and 4-Hydroxynonenal Adducts to Radical-Scavenging Soy Peptides. *J. Agric. Food Chem.* **2012**, *60*, 9727–9736.
- (37) Keller, A.; Nesvizhskii, A. I.; Kolker, E.; Aebersold, R. Empirical Statistical Model To Estimate the Accuracy of Peptide Identifications Made by MS/MS and Database Search. *Anal. Chem.* **2002**, *74*, 5383–5392.
- (38) Searle, B. C.; Turner, M.; Nesvizhskii, A. I. Improving Sensitivity by Probabilistically Combining Results from Multiple MS/MS Search Methodologies. *J. Proteome Res.* **2008**, *7*, 245–253.
- (39) Käll, L.; Storey, J. D.; MacCoss, M. J.; Noble, W. S. Assigning Significance to Peptides Identified by Tandem Mass Spectrometry Using Decoy Databases. *J. Proteome Res.* **2008**, *7*, 29–34.
- (40) Nesvizhskii, A. I.; Keller, A.; Kolker, E.; Aebersold, R. A Statistical Model for Identifying Proteins by Tandem Mass Spectrometry. *Anal. Chem.* **2003**, *75*, 4646–4658.
- (41) Ishii, T.; Kumazawa, S.; Sakurai, T.; Nakayama, T.; Uchida, K. Mass Spectroscopic Characterization of Protein Modification by Malondialdehyde. *Chem. Res. Toxicol.* **2006**, *19*, 122–129.
- (42) Žídek, L.; Doležel, P.; Chmelík, J.; Baker, A. G.; Novotny, M. Modification of Horse Heart Cytochrome c with Trans-2-Hexenal. *Chem. Res. Toxicol.* **1997**, *10*, 702–710.
- (43) Bruenner, B. A.; Daniel Jones, A.; Bruce German, J. Maximum Entropy Deconvolution of Heterogeneity in Protein Modification: Protein Adducts of 4-Hydroxy-2-Nonenal. *Rapid Commun. Mass Spectrom.* **1994**, *8*, 509–512.
- (44) Bruenner, B. A.; Jones, A. D.; German, J. B. Direct Characterization of Protein Adducts of the Lipid Peroxidation Product 4-Hydroxy-2-Nonenal Using Electrospray Mass Spectrometry. *Chem. Res. Toxicol.* **1995**, *8*, 552–559.
- (45) Smathers, R. L.; Fritz, K. S.; Galligan, J. J.; Shearn, C. T.; Reigan, P.; Marks, M. J.; Petersen, D. R. Characterization of 4-HNE Modified L-FABP Reveals Alterations in Structural and Functional Dynamics. *PLoS One* **2012**, *7*, No. e38459.
- (46) Sayre, L. M.; Arora, P. K.; Iyer, R. S.; Salomon, R. G. Pyrrole Formation from 4-Hydroxynonenal and Primary Amines. *Chem. Res. Toxicol.* **1993**, *6*, 19–22.
- (47) Jumper, J.; Evans, R.; Pritzel, A.; Green, T.; Figurnov, M.; Ronneberger, O.; Tunyasuvunakool, K.; Bates, R.; Žídek, A.; Potapenko, A.; Bridgland, A.; Meyer, C.; Kohl, S. A. A.; Ballard, A. J.; Cowie, A.; Romera-Paredes, B.; Nikolov, S.; Jain, R.; Adler, J.; Back, T.; Petersen, S.; Reiman, D.; Clancy, E.; Zielinski, M.; Steinegger, M.; Pacholska, M.; Berghammer, T.; Bodenstein, S.; Silver, D.; Vinyals, O.; Senior, A. W.; Kavukcuoglu, K.; Kohli, P.; Hassabis, D. Highly Accurate Protein Structure Prediction with AlphaFold. *Nature* **2021**, *596*, 583–589.
- (48) Varadi, M.; Anyango, S.; Deshpande, M.; Nair, S.; Natassia, C.; Yordanova, G.; Yuan, D.; Stroe, O.; Wood, G.; Laydon, A.; Žídek, A.; Green, T.; Tunyasuvunakool, K.; Petersen, S.; Jumper, J.; Clancy, E.; Green, R.; Vora, A.; Lutfi, M.; Figurnov, M.; Cowie, A.; Hobbs, N.; Kohli, P.; Kleywegt, G.; Birney, E.; Hassabis, D.; Velankar, S. AlphaFold Protein Structure Database: Massively Expanding the Structural Coverage of Protein-Sequence Space with High-Accuracy Models. *Nucleic Acids Res.* **2022**, *50*, D439–D444.
- (49) Mirdita, M.; Schütze, K.; Moriwaki, Y.; Heo, L.; Ovchinnikov, S.; Steinegger, M. ColabFold: Making Protein Folding Accessible to All. *Nat. Methods* **2022**, *19*, 679–682.
- (50) Pejaver, V.; Urresti, J.; Lugo-Martinez, J.; Pagel, K. A.; Lin, G. N.; Nam, H.-J.; Mort, M.; Cooper, D. N.; Sebat, J.; Iakoucheva, L. M.; Mooney, S. D.; Radivojac, P. Inferring the Molecular and Phenotypic Impact of Amino Acid Variants with MutPred2. *Nat. Commun.* **2020**, *11*, No. 5918.
- (51) Dill, K. A.; MacCallum, J. L. The Protein-Folding Problem, 50 Years On. *Science* **2012**, *338*, 1042–1046.
- (52) Nick Pace, C.; Scholtz, J. M.; Grimsley, G. R. Forces Stabilizing Proteins. *FEBS Lett.* **2014**, *588*, 2177–2184.
- (53) Newberry, R. W.; Raines, R. T. Secondary Forces in Protein Folding. *ACS Chem. Biol.* **2019**, *14*, 1677–1686.
- (54) Spickett, C. M.; Pitt, A. R. Modification of Proteins by Reactive Lipid Oxidation Products and Biochemical Effects of Lipoxidation. *Essays Biochem.* **2020**, *64*, 19–31.
- (55) Castro, J. P.; Jung, T.; Grune, T.; Siems, W. 4-Hydroxynonenal (HNE) Modified Proteins in Metabolic Diseases. *Free Radicals Biol. Med.* **2017**, *111*, 309–315.
- (56) Jové, M.; Mota-Martorell, N.; Pradas, I.; Martín-Gari, M.; Ayala, V.; Pamplona, R. The Advanced Lipoxidation End-Product Malondialdehyde-Lysine in Aging and Longevity. *Antioxidants* **2020**, *9*, No. 1132.

- (57) Chavez, J.; Chung, W.-G.; Miranda, C. L.; Singhal, M.; Stevens, J. F.; Maier, C. S. Site-Specific Protein Adducts of 4-Hydroxy-2(E)-Nonenal in Human THP-1 Monocytic Cells: Protein Carbonylation Is Diminished by Ascorbic Acid. *Chem. Res. Toxicol.* **2010**, *23*, 37–47.
- (58) Griesser, E.; Vemula, V.; Mónico, A.; Pérez-Sala, D.; Fedorova, M. Dynamic Posttranslational Modifications of Cytoskeletal Proteins Unveil Hot Spots under Nitroxidative Stress. *Redox Biol.* **2021**, *44*, No. 102014.
- (59) Aldini, G.; Dalle-Donne, I.; Vistoli, G.; Maffei Facino, R.; Carini, M. Covalent Modification of Actin by 4-Hydroxy-Trans-2-Nonenal (HNE): LC-ESI-MS/MS Evidence for Cys374 Michael Addition. *J. Mass Spectrom.* **2005**, *40*, 946–954.
- (60) Camarillo, J. M.; Ullery, J. C.; Rose, K. L.; Marnett, L. J. Electrophilic Modification of PKM2 by 4-Hydroxynonenal and 4-Oxononenal Results in Protein Cross-Linking and Kinase Inhibition. *Chem. Res. Toxicol.* **2017**, *30*, 635–641.
- (61) Corso, A. D.; Monte, M. D.; Vilardo, P. G.; Cecconi, I.; Moschini, R.; Banditelli, S.; Cappiello, M.; Tsai, L.; Mura, U. Site-Specific Inactivation of Aldose Reductase by 4-Hydroxynonenal. *Arch. Biochem. Biophys.* **1998**, *350*, 245–248.
- (62) Reed, T.; Perluigi, M.; Sultana, R.; Pierce, W. M.; Klein, J. B.; Turner, D. M.; Coccia, R.; Markesberry, W. R.; Butterfield, D. A. Redox Proteomic Identification of 4-Hydroxy-2-Nonenal-Modified Brain Proteins in Amnestic Mild Cognitive Impairment: Insight into the Role of Lipid Peroxidation in the Progression and Pathogenesis of Alzheimer's Disease. *Neurobiol. Dis.* **2008**, *30*, 107–120.
- (63) Carbone, D. L.; Doorn, J. A.; Kiebler, Z.; Sampey, B. P.; Petersen, D. R. Inhibition of Hsp72-Mediated Protein Refolding by 4-Hydroxy-2-Nonenal. *Chem. Res. Toxicol.* **2004**, *17*, 1459–1467.
- (64) Carbone, D. L.; Doorn, J. A.; Kiebler, Z.; Ickes, B. R.; Petersen, D. R. Modification of Heat Shock Protein 90 by 4-Hydroxynonenal in a Rat Model of Chronic Alcoholic Liver Disease. *J. Pharmacol. Exp. Ther.* **2005**, *315*, 8–15.
- (65) Liu, W.; Akhand, A. A.; Kato, M.; Yokoyama, I.; Miyata, T.; Kurokawa, K.; Uchida, K.; Nakashima, I. 4-Hydroxynonenal Triggers an Epidermal Growth Factor Receptor-Linked Signal Pathway for Growth Inhibition. *J. Cell Sci.* **1999**, *112*, 2409–2417.
- (66) Ji, C.; Kozak, K. R.; Marnett, L. J. IkB Kinase, a Molecular Target for Inhibition by 4-Hydroxy-2-Nonenal\*. *J. Biol. Chem.* **2001**, *276*, 18223–18228.
- (67) Suzuki, T.; Muramatsu, A.; Saito, R.; Iso, T.; Shibata, T.; Kuwata, K.; Kawaguchi, S.; Iwawaki, T.; Adachi, S.; Suda, H.; Morita, M.; Uchida, K.; Baird, L.; Yamamoto, M. Molecular Mechanism of Cellular Oxidative Stress Sensing by Keap1. *Cell Rep.* **2019**, *28*, 746–758.e4.
- (68) Covey, T. M.; Edes, K.; Coombs, G. S.; Virshup, D. M.; Fitzpatrick, F. A. Alkylation of the Tumor Suppressor PTEN Activates Akt and  $\beta$ -Catenin Signaling: A Mechanism Linking Inflammation and Oxidative Stress with Cancer. *PLoS One* **2010**, *5*, No. e13545.
- (69) Di Domenico, F.; Tramutola, A.; Barone, E.; Lanzillotta, C.; Defever, O.; Arena, A.; Zuliani, I.; Foppoli, C.; Iavarone, F.; Vincenzoni, F.; Castagnola, M.; Butterfield, D. A.; Perluigi, M. Restoration of Aberrant MTOR Signaling by Intranasal Rapamycin Reduces Oxidative Damage: Focus on HNE-Modified Proteins in a Mouse Model of down Syndrome. *Redox Biol.* **2019**, *23*, No. 101162.
- (70) Shearn, C. T.; Fritz, K. S.; Reigan, P.; Petersen, D. R. Modification of Akt2 by 4-Hydroxynonenal Inhibits Insulin-Dependent Akt Signaling in HepG2 Cells. *Biochemistry* **2011**, *50*, 3984–3996.
- (71) Shearn, C. T.; Smathers, R. L.; Backos, D. S.; Reigan, P.; Orlicky, D. J.; Petersen, D. R. Increased Carbonylation of the Lipid Phosphatase PTEN Contributes to Akt2 Activation in a Murine Model of Early Alcohol-Induced Steatosis. *Free Radicals Biol. Med.* **2013**, *65*, 680–692.
- (72) Aldini, G.; Regazzoni, L.; Orioli, M.; Rimoldi, I.; Facino, R. M.; Carini, M. A Tandem MS Precursor-Ion Scan Approach to Identify Variable Covalent Modification of Albumin Cys34: A New Tool for Studying Vascular Carbonylation. *J. Mass Spectrom.* **2008**, *43*, 1470–1481.
- (73) Del Rio, D.; Stewart, A. J.; Pellegrini, N. A Review of Recent Studies on Malondialdehyde as Toxic Molecule and Biological Marker of Oxidative Stress. *Nutr., Metab. Cardiovasc. Dis.* **2005**, *15*, 316–328.
- (74) AMSA. *Meat Color Measurement Guidelines*; The American Meat Science Association (AMSA): Champaign, IL, 2012.
- (75) Elroy, N. N.; Rogers, J.; Mafi, G. G.; VanOverbeke, D. L.; Hartson, S. D.; Ramanathan, R. Species-Specific Effects on Non-Enzymatic Metmyoglobin Reduction in Vitro. *Meat Sci.* **2015**, *105*, 108–113.
- (76) Lynch, M. P.; Faustman, C. Effect of Aldehyde Lipid Oxidation Products on Myoglobin. *J. Agric. Food Chem.* **2000**, *48*, 600–604.
- (77) Ramanathan, R.; Mancini, R. A.; Suman, S. P.; Cantino, M. E. Effects of 4-Hydroxy-2-Nonenal on Beef Heart Mitochondrial Ultrastructure, Oxygen Consumption, and Metmyoglobin Reduction. *Meat Sci.* **2012**, *90*, 564–571.
- (78) Geesink, G. H.; Kuchay, S.; Chishti, A. H.; Koohmariae, M.  $\mu$ -Calpain Is Essential for Postmortem Proteolysis of Muscle Proteins<sup>1,2</sup>. *J. Anim. Sci.* **2006**, *84*, 2834–2840.
- (79) Liu, R.; Li, Y.; Wang, M.; Zhou, G.; Zhang, W. Effect of Protein S-Nitrosylation on Autolysis and Catalytic Ability of  $\mu$ -Calpain. *Food Chem.* **2016**, *213*, 470–477.
- (80) Liu, P.; Zhang, Z.; Guo, X.; Zhu, X.; Mao, X.; Guo, X.; Deng, X.; Zhang, J.  $\mu$ -Calpain Oxidation and Proteolytic Changes on Myofibrillar Proteins from Coregonus Peled in Vitro. *Food Chem.* **2021**, *361*, No. 130100.
- (81) Boehm, M. L.; Kendall, T. L.; Thompson, V. F.; Goll, D. E. Changes in the Calpains and Calpastatin during Postmortem Storage of Bovine Muscle. *J. Anim. Sci.* **1998**, *76*, 2415.
- (82) Melody, J. L.; Lonergan, S. M.; Rowe, L. J.; Huiatt, T. W.; Mayes, M. S.; Huff-Lonergan, E. Early Postmortem Biochemical Factors Influence Tenderness and Water-Holding Capacity of Three Porcine Muscles. *J. Anim. Sci.* **2004**, *82*, 1195–1205.
- (83) Zalewska, T.; Thompson, V. F.; Goll, D. E. Effect of Phosphatidylinositol and Inside-out Erythrocyte Vesicles on Autolysis of  $\mu$ - and m-Calpain from Bovine Skeletal Muscle. *Biochim. Biophys. Acta, Mol. Cell Res.* **2004**, *1693*, 125–133.
- (84) Cottin, P.; Poussard, S.; Desmazes, J. P.; Georgescauld, D.; Ducastaing, A. Free Calcium and Calpain I Activity. *Biochim. Biophys. Acta, Protein Struct. Mol. Enzymol.* **1991**, *1079*, 139–145.
- (85) Zimmerman, U.-J. P.; Schlaepfer, W. W. Two-Stage Autolysis of the Catalytic Subunit Initiates Activation of Calpain I. *Biochim. Biophys. Acta, Protein Struct. Mol. Enzymol.* **1991**, *1078*, 192–198.
- (86) Chen, L.; Zhou, G.; Zhang, W. Effects of High Oxygen Packaging on Tenderness and Water Holding Capacity of Pork Through Protein Oxidation. *Food Bioprocess Technol.* **2015**, *8*, 2287–2297.
- (87) Fu, Q.-q.; Ge, Q.; Liu, R.; Wang, H.; Zhou, G.; Zhang, W. Influence of Modified Atmosphere Packaging on Protein Oxidation, Calpain Activation and Desmin Degradation of Beef Muscles. *J. Sci. Food Agric.* **2017**, *97*, 4508–4514.
- (88) Argyri, A. A.; Mallouchos, A.; Panagou, E. Z.; Nychas, G.-J. E. The Dynamics of the HS/SPME–GC/MS as a Tool to Assess the Spoilage of Minced Beef Stored under Different Packaging and Temperature Conditions. *Int. J. Food Microbiol.* **2015**, *193*, 51–58.
- (89) Fritz, K. S.; Kellersberger, K. A.; Gomez, J. D.; Petersen, D. R. 4-HNE Adduct Stability Characterized by Collision-Induced Dissociation and Electron Transfer Dissociation Mass Spectrometry. *Chem. Res. Toxicol.* **2012**, *25*, 965–970.
- (90) Benyamin, Y. The Structural Basis of Calpain Behavior. *FEBS J.* **2006**, *273*, 3413–3414.